# ANALYSIS OF NITROGEN IMPURITY IMPACT ON $^{14}C$ GENERATION IN RBMK-1500 REACTOR GRAPHITE

Ernestas Narkunas, Arturas Smaizys, Povilas Poskas
Lithuanian Energy Institute, Breslaujos 3, LT-44403 Kaunas, Lithuania

## ABSTRACT

There are two RBMK-1500 water-cooled graphite-moderated channel-type power reactors at Ignalina Nuclear Power Plant (INPP). The total mass of graphite in the cores of both units at INPP is more than 3600 tons. Knowledge of the radiological characteristics and radioactive inventory of irradiated graphite are essential in planning of the decommissioning processes and in the choice of graphite treatment, storage and disposal methods.

The main source of uncertainty in the assessment of graphite activity is the uncertainty of the initial impurities content in graphite. Nitrogen is one of the most important impurities in the graphite. Having large neutron capture cross-section this impurity may become dominant source of $^{14}C$ generation in graphite. Furthermore, RBMK reactors graphite stacks operate in the cooling mixture of helium-nitrogen gases and this may additionally increase the quantity of nitrogen impurity in graphite.

The numerical modelling of graphite activation was performed for Ignalina NPP Unit 1 reactor. The composition of radionuclides in the irradiated graphite was evaluated on the basis of the modelled neutron fluxes (computer code MCNP 5) using ORIGEN-S code from SCALE 5 codes system and Ignalina NPP Unit 1 reactor operation history. Several cases with different nitrogen content were modelled in order to evaluate $^{14}C$ activity dependence on initial nitrogen impurity content.

## INTRODUCTION

Ignalina Nuclear Power Plant (INPP) Unit 1 was shut down at the end of 2004. Unit 1 contains RBMK-1500 water-cooled graphite-moderated channel-type power reactor. Cross section of RBMK-1500 reactor vault is presented in Fig. 1 [1]. The graphite stack (6) serves as a neutron moderator and reflector. The graphite stack consist of individual graphite blocks (16) made of GR-280 grade graphite and can be visualized as a vertical cylinder, made up of 2488 graphite columns (8 m height), constructed from different types of graphite blocks. The upper 0.5 m thick graphite stack layer is called top reflector whereas the lower 0.5 m thick layer is bottom reflector. The blocks are rectangular parallelepipeds, with a base of 0.25 × 0.25 m, and heights of 0.2, 0.3 and 0.6 m. The blocks have a 0.114 m diameter bore openings through the vertical axis, and this provides a total of 2044 fuel (technological) channels (14) which are used for placing fuel assemblies (15), control rods and other equipment into the core. The openings in the remaining 444 peripheral graphite columns are filled with graphite rods in order to increase neutron reflection and these columns serves as radial reflector. In order to improve heat transfer from the graphite stack, the central segment of the fuel channel is surrounded by the 0.02 m high and 0.0115 m thick split GRP-2-125 grade graphite rings (17). These rings are arranged next to one another in such a manner that one is in contact with the channel, and the other with the graphite stack block. The graphite stack, including its hermetically sealed cavity, is called the sealed reactor space. This space is filled with a circulating helium-nitrogen mixture at an excess pressure of 0.49–1.96 kPa.

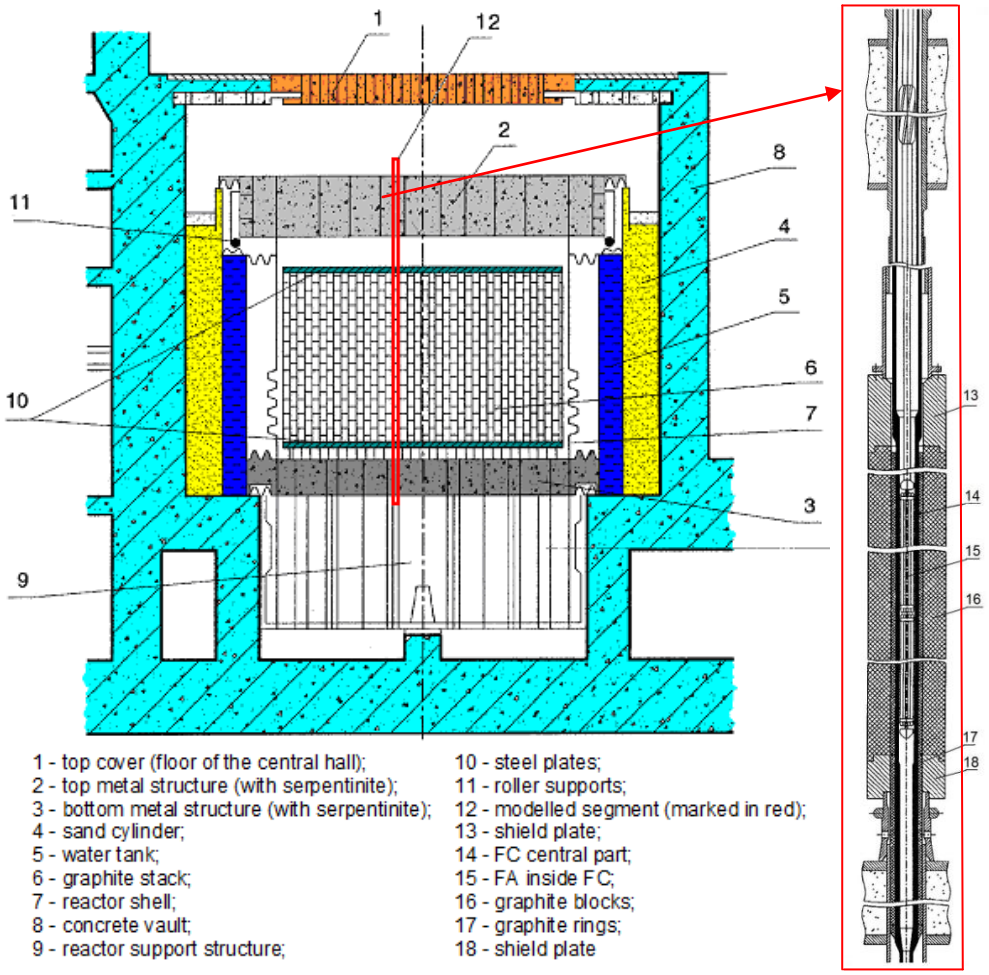


Fig. 1. Cross-section of RBMK-1500 reactor vault [1]

During reactor operation the graphite blocks and rings are under intensive neutron irradiation and became activated. One of the most important radionuclides in the activated RBMK-1500 reactors graphite is a long-lived $^{14}C$ [2, 3]. This radionuclide in RBMK reactor graphite may be generated mainly in two different ways: from activation of raw graphite material – carbon (through $^{13}C(n,\gamma)^{14}C$ reaction) and from activation of nitrogen impurities (through $^{14}N(n,p)^{14}C$ reaction). The generation of $^{14}C$ from oxygen activation is not significant for RBMK reactors, due to the small $^{17}O(n,\alpha)^{14}C$ reaction cross-section (~10 times lower than cross-section of $^{14}N(n,p)^{14}C$ reaction), small quantity of oxygen impurity in RBMK graphite matrix ($1.8\times10^{-4}$ % of mass for GR-280 grade graphite) with very little abundance of $^{17}O$ isotope in natural oxygen (0.04 %) and absence of oxygen in RBMK reactor cooling gas (maximal allowed volumetric concentration of oxygen in cooling gas is 0.005 % [8]). The fraction of generated $^{14}C$ from the raw carbon activation may be calculated quite precisely as the quantity of carbon in graphite is almost invariant and comprises more than 99.9 % of mass, while the fraction coming from nitrogen activation may differ depending on initial nitrogen impurity content. Furthermore, the adsorption of cooling helium-nitrogen gas mixture in graphite pores may additionally increase the quantity of nitrogen impurity and consequently increase $^{14}C$ generation.

The intention of this paper is to present modelling results of nitrogen impact to the $^{14}C$ generation in Ignalina NPP Unit 1 RBMK-1500 reactor's graphite blocks and rings.

## METHODOLOGY

Generally, the assessment of neutron induced activities requires, as a first step, the knowledge of the spatial and energy distributions of the neutron flux throughout the analysed

reactor system/component. The neutron flux is then used for the calculation of that component activity from the known concentration of the initial elements in the component's material.

In this study, the modelling of neutron fluxes distributions in the graphite structures is performed firstly. Then activation modelling of graphite structures is performed using already modelled neutron fluxes and distribution of $^{14}C$ activity in these structures along the reactor axis is obtained. And then the influence of nitrogen impurity content on generated $^{14}C$ activity in graphite blocks and rings is analysed at the points with the highest $^{14}C$ activity.

*Initial material composition*

Minimal and maximal concentrations of all impurities (taken from published sources ([4–7] for graphite blocks and [3, 6, 7] for graphite rings)) were used when modelling axial $^{14}C$ activities distributions. Then for modelling of nitrogen influence on $^{14}C$ generation no other impurities were taken into account and initial nitrogen content in graphite components was chosen 0 % of mass, i.e. pure graphite (carbon). After that several modelling cases were developed with different initial nitrogen impurity content up to 0.05 % of mass. It was always assumed that the isotopic composition of each chemical element is the same as the naturally occurring isotopic content.

*Modelling of spatial and energetic distribution of neutron flux*

A general methodology used for neutron fluxes modelling in the RBMK-1500 reactor graphite structures is presented in Fig. 2. The neutron fluxes modelling requires the input of reactor operation parameters, geometrics with specific material compositions, cross-sections for neutrons transport and appropriate neutrons transport modelling code. MCNP 5 computer code was used for neutron flux modelling, as this code successfully solves neutron transport problems practically in any 3D geometries and materials configuration.

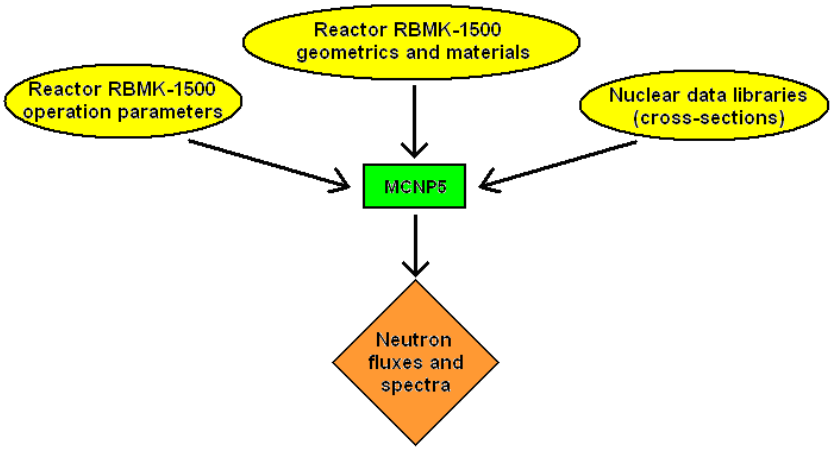


Fig. 2. A general methodology of neutron fluxes modelling

Various data of RBMK-1500 reactor were used while developing MCNP model. These data are: geometrics of reactor components, materials compositions and densities, reactor operation parameters and etc. These data were based on the information presented in ref. [1, 8, 9].

From the beginning of its operation in 1984, INPP Unit 1 RBMK-1500 reactor was loaded with $UO_2$ fuel having 2.0 % $^{235}U$ initial enrichment. Later, starting from 1997 $UO_2$ fuel with 2.4 % $^{235}U$ enrichment and 0.41 % burnable $Er_2O_3$ absorber content was introduced and from 2002 $UO_2$ fuel with 2.6 % $^{235}U$ enrichment and 0.5 % burnable $Er_2O_3$ absorber content was introduced. When reactor is in operation the fuel burns up and fuel assemblies with burned fuel are continuously replaced with the assemblies having fresh fuel. According to [9], the average

fuel burnup in the reactor is in the range of 10–11 MWd/kgU. Taking into the consideration the information on the usage of nuclear fuel with different enrichment, burnable absorber content, the information on the average fuel burnup within reactor core ant the fact, that when evaluating neutron activation of reactor components, the neutron fluxes representing average reactor operation conditions during its whole lifetime should be used, the neutron flux modelling was performed assuming that:

- Fuel channel is loaded with $UO_2$ fuel of average burnup of ~10 MWd/kgU with 2.4 % $^{235}U$ initial enrichment and 0.41 % burnable $Er_2O_3$ absorber;

The radionuclide inventory of irradiated fuel (2.4 % $^{235}U$ enrichment and 0.41 % burnable $Er_2O_3$ absorber with burnup up to ~10 MWd/kgU) was modelled with computer code SAS2 from SCALE 5 computer codes system. The remaining reactor operation parameters were set corresponding to the average power fuel channel (~2.6 MW) working conditions.

A view of horizontal cross-section of one lattice segment model (0.25 × 0.25 m) of the Ignalina NPP RBMK-1500 reactor, developed with MCNP 5 code, is presented in Fig. 3. This model of one reactor lattice cell segment, using periodic boundary conditions for the side walls of the segment, corresponds to an infinite lattice comprised of such segments and is suitable for modelling of neutron fluxes in the reactor construction elements of central (in radial direction) core part (plateau). This approach for estimation of neutron fluxes is conservative (gives higher neutron fluxes) because the impact of technological channels with control rods (or with other equipment, or even empty, i.e. filled only with coolant) in the vicinity of analyzed segment is not taken into account.

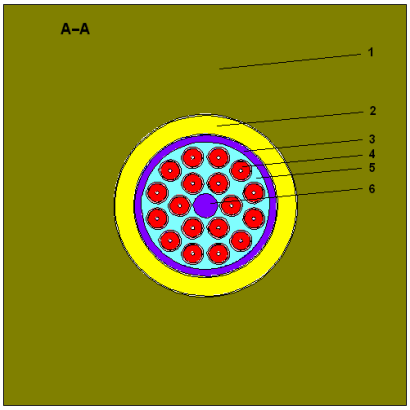


Fig. 3. Cross-section of modelled segment of RBMK-1500 reactor (throughout fuel bundle)

1 - Graphite block; 3 - Fuel channel (FC); 5 - Coolant (steam-water mixture);
2 - Graphite ring; 4 - Fuel element; 6 - FA central rod

In order to evaluate the characteristics of the neutron fluxes, their differences and axial variation, modelled graphite structures (blocks and sleeves) were subdivided in to several separate zones in reactor axial direction and neutron fluxes were estimated in each of them. Modelling the neutron fluxes in this manner and analysing their axial variation allows properly divide these reactor constructions into different zones with different activation conditions and perform adequate evaluation of their activation.

The estimated neutron fluxes with MCNP were grouped into three energy groups:

- Thermal neutrons, with energies up to 0.625 eV;
- Resonance neutrons, with energies in range of 0.625 eV – 1 MeV;
- Fast neutrons, with energies above 1 MeV.

This was done keeping in mind, that results of this estimation are used in the second step of neutron activation modelling of reactor graphite components, i.e. induced activity modelling

with ORIGEN-S computer code, which uses specifically those energy group ranges for neutron fluxes input.

*Modelling of the neutron activation of the reactor components*

A general methodology used for neutron activation modelling is presented in Fig. 4.

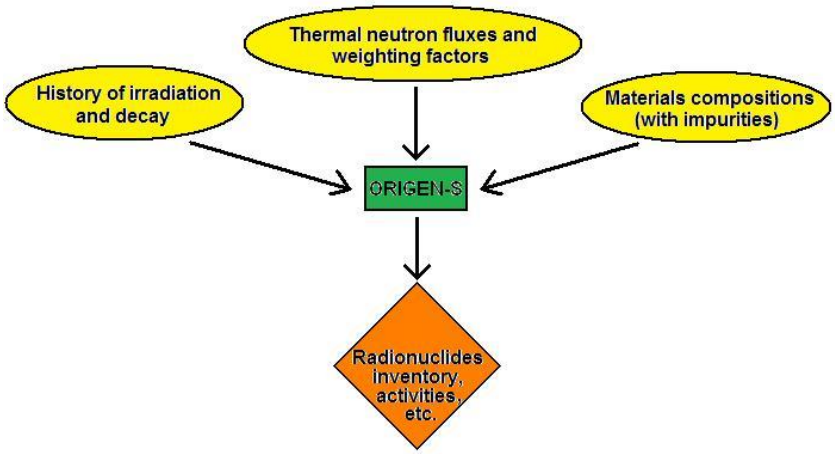


Fig. 4. A general methodology of neutron activation modelling

ORIGEN-S computer code from SCALE 5 codes system, that is validated and verified for analysis of such processes and is widely used in the world, was used for the activation estimation. The code considers radioactive disintegration and neutron absorption (capture and fission) and enables to identify isotopic content, activities and concentrations of neutron activated elements. The time rate of the change of the concentration for a particular nuclide $N_i$ can be written as:

$$\frac{dN_i}{dt} = \sum_j \gamma_{ji}\sigma_{f,j}N_j\phi + \sigma_{c,i-1}N_{i-1}\phi + \lambda_i^{'}N_i^{'} - \sigma_{f,i}N_i\phi - \sigma_{c,i}N_i\phi - \lambda_i N_i, \quad i = 1,...I \ ,$$

where:

$\sum_j \gamma_{ji}\sigma_{f,j}N_j\phi$ – the yield rate of $N_i$ due to the fission of all nuclides $N_j$;

$\sigma_{c,i-1}N_{i-1}\phi$ – the rate of transmutation into $N_i$, due to neutron capture by nuclide $N_{i-1}$;

$\lambda_i^{'}N_i^{'}$ – the rate of formation of $N_i$ due to the radioactive decay of nuclides $N_i^{'}$;

$\sigma_{f,i}N_i\phi$ – the destruction rate of $N_i$ due to fission;

$\sigma_{c,i}N_i\phi$ – the destruction rate of $N_i$ due to all forms of neutron absorption other than fission (n, γ), (n, α), (n, p), (n, 2n) (n, 3n);

$\lambda_i N_i$ – the radioactive decay rate of $N_i$.

When running ORIGEN-S as a stand-alone module, the input data associated with neutron fluxes are thermal neutron flux and the cross-section weighting factors THERM, RES, and FAST. Factor THERM may be determined using the moderator temperature while RES and FAST are calculated as the ratio of the resonance energy flux to the thermal flux and the ratio of the fast energy flux to the thermal flux respectively.

The real operating history of Ignalina NPP reactor Unit 1 was used for the neutron activation modelling (see Fig. 5 and Fig. 6). It was assumed that for the first 17 years (17 cycles) reactor operates at different regimes continuously without shutdowns (see Fig. 5), but during each cycle (one cycle corresponds to the one year period) operation regime remains constant. In

order to evaluate activation more precisely, remaining 4 years of operation were divided into 25 shorter periods taking into account all reactor shutdowns, as presented in Fig. 6.

As the reactor thermal power directly corresponds to the thermal neutron flux, thermal neutron fluxes for each separate cycle (used in ORIGEN-S modelling) were recalculated according to the reactor thermal power during that cycle and the neutron flux modelled for reactor operation at 4200 MW thermal power (~2.6 MW for one FC).

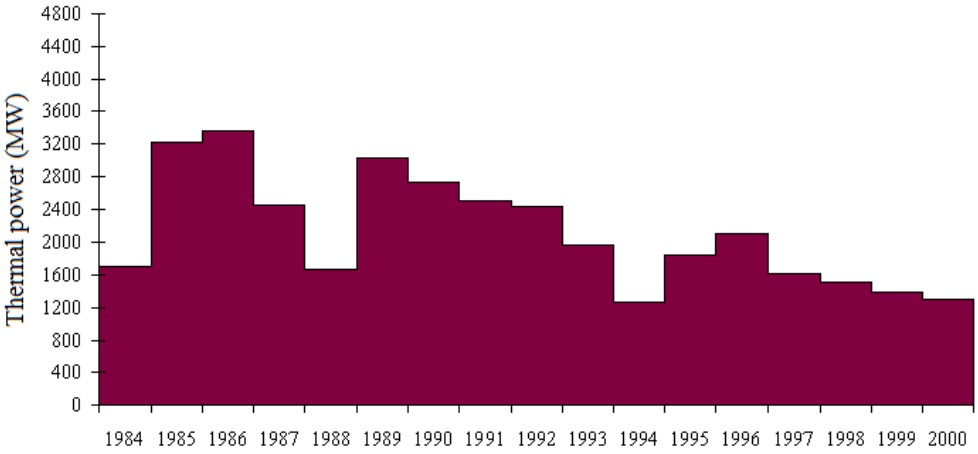


Fig. 5. The Ignalina NPP Unit 1 reactor operation history data for 1984 – 2000

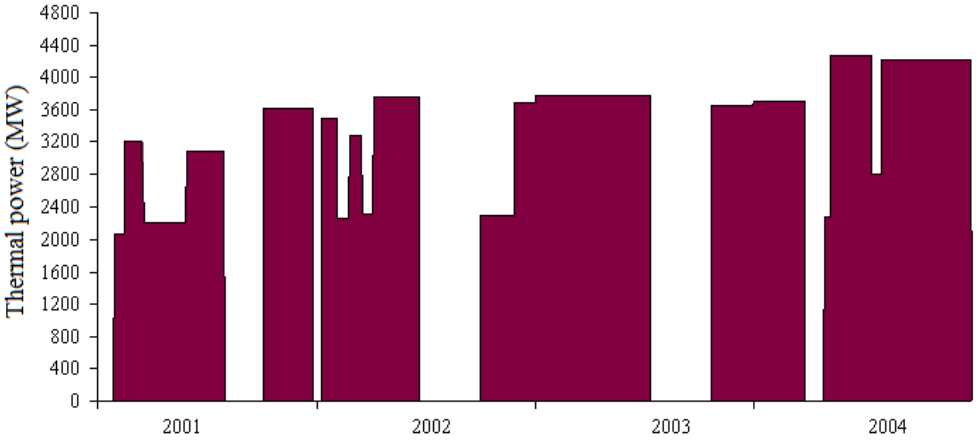


Fig. 6. The Ignalina NPP Unit 1 reactor operation history data for 2001 – 2004

## RESULTS AND DISCUSSION

### *Spatial and energetic neutron flux distribution*

Modelled neutron fluxes in the RBMK-1500 reactor graphite blocks and rings for RBMK-1500 reactor 4200 MW thermal power operation are presented in Fig. 7. For convenience purpose the axial distance from the centre of the reactor core is given in the ordinate axis, assuming that the centre is at zero mark.

The results of the neutron flux modelling show that thermal and resonance neutron fluxes are dominant in the graphite blocks and rings; however, thermal neutron flux is more intensive than resonance neutron in the graphite blocks (though very insignificantly in certain regions), whereas, resonance neutron flux is more intensive than thermal in graphite rings (except the very centre, top and bottom reflectors regions), see Fig. 7.

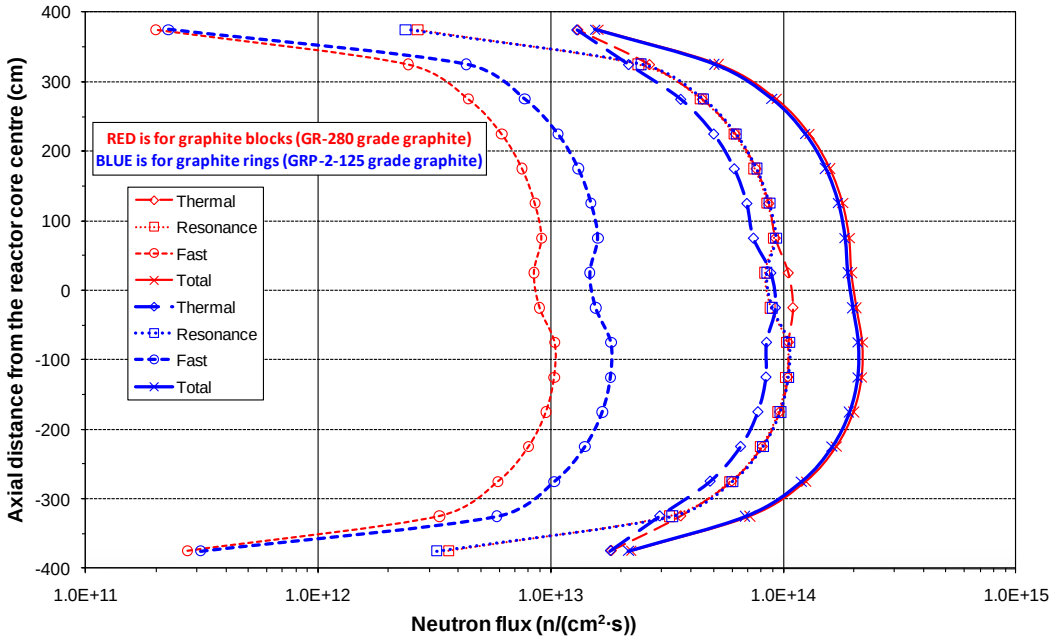


Fig. 7. Neutron fluxes in the graphite blocks and rings

The fast neutron flux is about 10 times lower than that of resonance neutrons and their distribution along the axial direction is the same as the resonance neutron flux variations in graphite blocks. There are two maximums in the distribution profile of the fast and resonance neutron fluxes and one minimum in the reactor core centre, which corresponds to the point of the fuel bundles connection in the fuel assembly. In this region the fast and resonance neutron fluxes are approx. 1.2 times lower than the maximal neutron fluxes. In the graphite blocks column edges (reflector blocks) the fast and resonance neutron fluxes are approx. 34 (top reflector) and 28 (bottom reflector) times lower than the maximal neutron fluxes. For thermal neutron flux there is only one maximum in the neutron flux distribution profile and it is located in the central part of the reactor core. Going further from the reactor core centre the thermal flux decrease monotonically and in the graphite column edges i.e. top and bottom reflectors is ~8 and ~6 times lower than the maximal flux, respectively.

Similar neutron fluxes distributions are obtained and for graphite rings in the reactor core. However, the fast neutron flux is about 6 times lower than that of resonance neutrons and the resonance neutron flux is dominant in the regions near the fuel bundles while the thermal flux is dominant in the top, central and bottom parts of the reactor core.

Comparison of neutron fluxes in the graphite bocks and rings gives, that total and resonance neutron fluxes are almost equal in these structures, but thermal neutron flux is about 1.2 times higher in blocks than in rings, whereas fast neutron flux is 1.8 times higher in rings.

*Graphite activation*

Modelled $^{14}C$ activity distribution in the graphite blocks and rings (using already modelled neutron fluxes, see Fig. 7) along the reactor axis after the reactor final shutdown (RFS) is presented in Fig. 8. $^{14}C$ activity distribution is almost identical in the graphite rings for minimal and maximal initial impurities concentrations. This is because there is no data on nitrogen impurities in GRP-2-125 grade graphite in published sources [3, 6, 7], thus nitrogen impurity was not used in modelling and all generated $^{14}C$ for graphite rings comes practically only from activation of carbon in both cases. However, it should be noted, that absence of nitrogen impurities data for GRP-2-125 grade graphite (in [3, 6, 7]) does not mean that there is no nitrogen impurities. Usually methods used for qualitative and quantitative impurities

determination are not suitable for nitrogen and other light elements and thus no data for these elements are provided.

For graphite blocks situation is different. For maximal initial impurities concentrations case $^{14}C$ activity is about 7 times higher than for minimal concentrations case. This difference is influenced mostly by nitrogen impurities in GR-280 grade graphite, because initial nitrogen concentration was $4\times10^{-5}$ % of mass [5] for minimal concentration case while for maximal concentrations case it was $7\times10^{-3}$ % of mass [7].

The modelling results also show that $^{14}C$ activity distribution along the axial direction in the graphite rings and blocks corresponds to the thermal neutron flux distribution (see Fig. 7 and Fig. 8) for all modelled cases. Maximal $^{14}C$ activity place coincides with the maximal thermal neutron flux place and (analogous to thermal flux) $^{14}C$ activity in the top and bottom parts is respectively ~8 and ~6 times lower than the maximal activity. This confirms the fact that generation of $^{14}C$ from carbon activation, as well as from nitrogen activation is determined by thermal neutron flux.

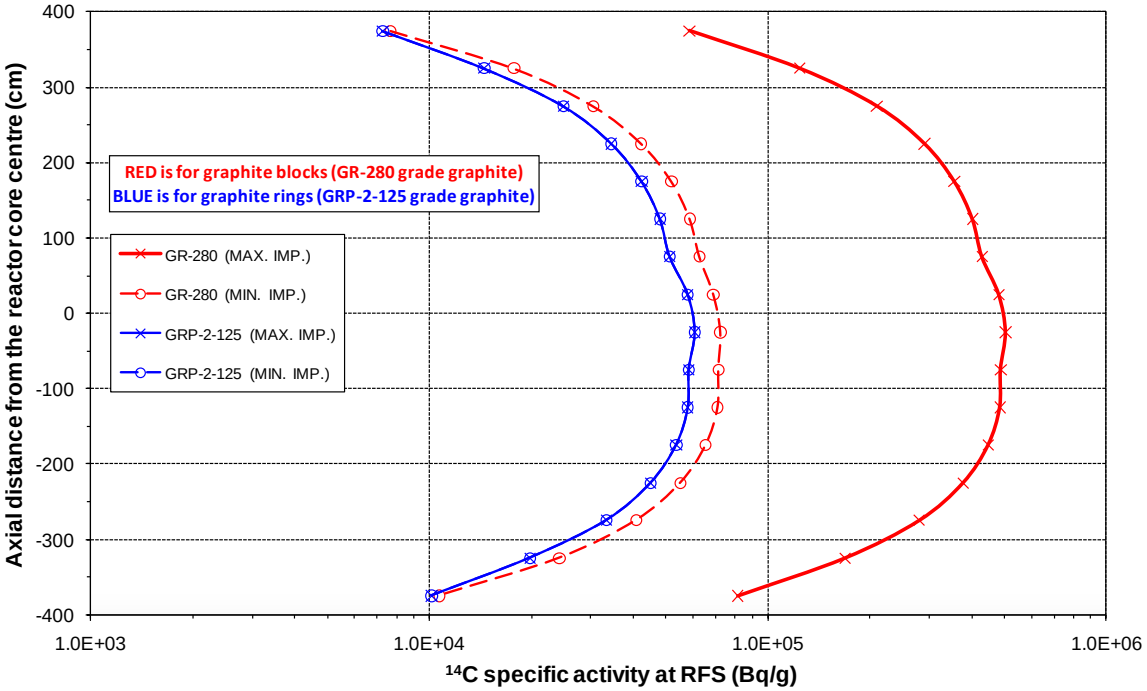


Fig. 8. $^{14}C$ activity distribution along reactor axis in graphite structures
MAX. IMP. – $^{14}C$ activity obtained using maximal concentrations of all impurities from published sources;
MIN. IMP. – $^{14}C$ activity obtained using minimal concentrations of all impurities from published sources

The place of maximal $^{14}C$ activity, as already mention above, coincides with the maximal thermal neutron flux place and is situated at 25 cm below the axial rector centre (elevation mark -25 cm in the Fig. 7 and Fig. 8). For this point, i.e. using modelled neutron fluxes in this place, the influence of nitrogen impurity content on generated $^{14}C$ activity in graphite blocks and rings was analysed and results of this analysis are presented in Fig. 9.

Fig. 9 shows total $^{14}C$ activity dependence on initial nitrogen impurity content in graphite blocks and rings, as well as separate ways of $^{14}C$ generation from carbon (raw material of graphite) and nitrogen (impurity). The generation of $^{14}C$ from carbon stays practically constant changing the nitrogen impurity content in analysed 0–0.5 % mass range, because the mass of main chemical element (carbon) in graphite practically stays unchanged. Activity of $^{14}C$ generated from carbon activation in this case comprises about $6\times10^{4}$ Bq/g in graphite rings and about $7\times10^{4}$ Bq/g in graphite blocks. This difference of activities is directly related to the thermal neutron flux differences in graphite blocks and rings, i.e. ~1.2 times higher activity in graphite blocks is due to the ~1.2 times higher thermal neutron flux in graphite blocks, compared to those in rings.

The generation of $^{14}C$ from nitrogen activation increases linear while increasing nitrogen content, and at ~$1\times10^{-3}$ % nitrogen mass concentration equals $^{14}C$ generation from carbon activation. The activity of $^{14}C$ generated from nitrogen activation (at the same initial concentration) in graphite blocks is also ~1.2 times higher than in graphite rings due to the mentioned differences of thermal neutron fluxes.

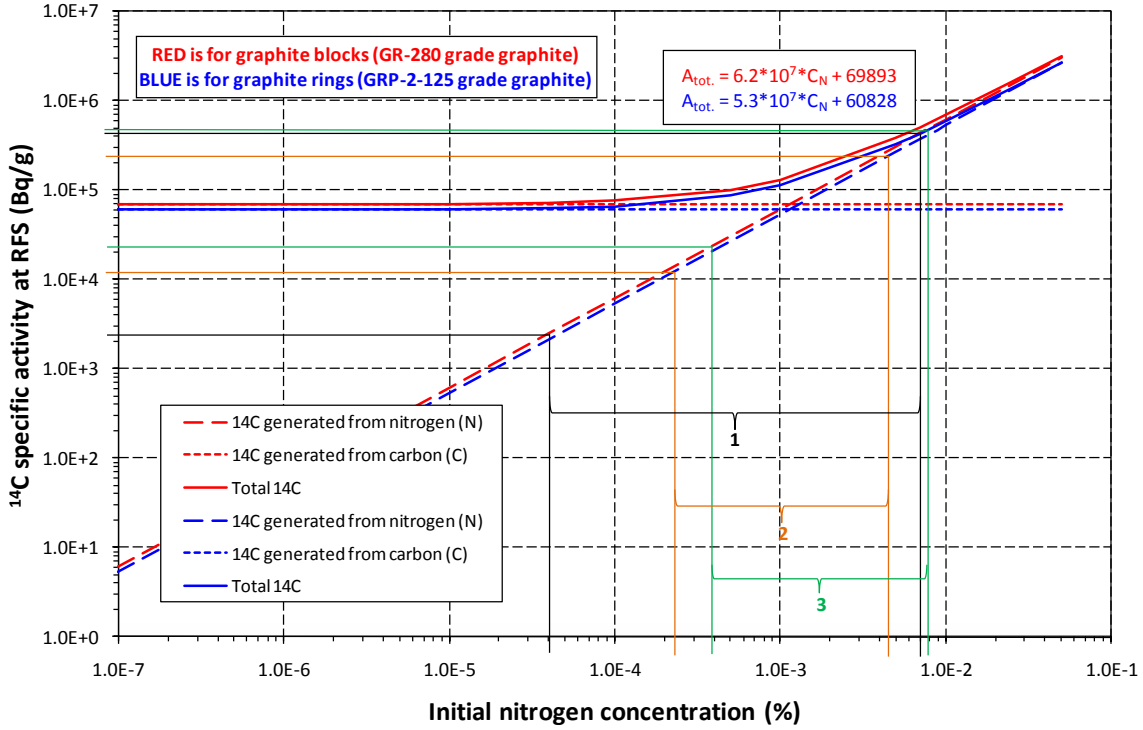


Fig. 9. $^{14}C$ activity dependence on initial nitrogen impurity concentration
Interval 1 – nitrogen concentration in GR-280 grade graphite matrix from published sources;
interval 2 – calculated nitrogen concentration in GRP-2-125 grade graphite pores;
interval 3 – calculated nitrogen concentration in GR-280 grade graphite pores

Modelling results show (Fig. 9), that for nitrogen impurity concentrations up to $1\times10^{-4}$ % mass, the activity of $^{14}C$ generated from nitrogen impurity activation is considerably lower than that of carbon activation and does not influences total $^{14}C$ activity. However, when nitrogen impurity concentration reaches $1\times10^{-3}$ % mass, the generation of $^{14}C$ from nitrogen activation equals the generation from carbon activation and with further increase of nitrogen concentration $^{14}N(n,p)^{14}C$ becomes dominant.

So, for nitrogen impurity concentrations from $4\times10^{-5}$ to $7\times10^{-3}$ % mass (marked as interval "1" in Fig. 9) in GR-280 grade graphite [4–7], the total activity of $^{14}C$ varies from ~$7\times10^{4}$ to ~$5\times10^{5}$ Bq/g where $^{14}C$ generated from carbon activation always comprises ~$7\times10^{4}$ Bq/g. There is no data on initial nitrogen impurity in GRP-2-125 grade graphite [3, 6, 7], however assuming that there can be the same nitrogen impurity concentration as in GR-280 grade graphite, the activity of total generated $^{14}C$ would be about 1.2 times lower than of GR-280 grade graphite and $^{14}C$ generated from carbon activation would comprise ~$6\times10^{4}$ Bq/g.

Published data on initial nitrogen impurities in graphite are for virgin unirradiated graphite and may be conservatively considered as impurities incorporated into the graphite matrix. However, graphite is a porous material and porosity of GR-280 grade graphite is about 23 % (17 % are for open and 6 % are for closed pores volume) [10], while porosity of GRP-2-125 grade graphite is about 16 % (14 % are for open and 2 % are for closed pores volume) [11]. As RBMK reactors graphite stack is cooled with mixture of helium-nitrogen gases, nitrogen can penetrate into the open graphite pores and additionally increase its concentration in graphite. Depending on reactor operation state nitrogen volumetric content in cooling gases may be in the range of 5–100 % and there are 3 basic cooling gas volumetric compositions [8, 9]:

- Dry air (where $N_2$ comprises about 80 %). This is for an auxiliary regime which is only used for a shutdown reactor.
- Nitrogen (100 % $N_2$). This is for an auxiliary regime which is used at the reactor power below 750 MW(e).
- Helium-nitrogen mixture (90 % He + 10 % $N_2$). This is for normal reactor power operation.

Taking into account the facts that cooling gases circulates in the rector sealed space at an excess pressure of 0.49 – 1.96 kPa and that gas temperature is about 350 $^{o}$C, the concentration of $N_2$ gas (number of $N_2$ molecules) in 1 $cm^3$ volume of 100 % $N_2$ gas cooling mode may be calculated using the ideal gas law (pV=nkT):

- for 0.49 kPa excess pressure:

$$n_1 = \frac{p_1 V}{kT} = \frac{(101325 + 490)[N/m^2] \times 1 \times 10^{-6}[m^3]}{1.38 \times 10^{-23}[N \times m/K] \times (350 + 273.15)[K]} = 1.18 \times 10^{19};$$

- for 1.96 kPa excess pressure:

$$n_2 = \frac{p_2 V}{kT} = \frac{(101325 + 1960)[N/m^2] \times 1 \times 10^{-6}[m^3]}{1.38 \times 10^{-23}[N \times m/K] \times (350 + 273.15)[K]} = 1.20 \times 10^{19};$$

where:

$n$ – number of $N_2$ gas molecules;
$p$ – pressure in Pa ($N/m^2$);
$V$ – volume in $m^3$ (for $1cm^3$ in our case it is $1 \times 10^{-6}$ $m^3$);
$k$ – Boltzmann's constant;
$T$ – gas temperature in K.

This shows that $N_2$ gas concentration in cooling gases varies insignificantly depending on operational pressure, however taking into account possible cooling gas volumetric composition (5–100 % of $N_2$ gases) and pressure, the concentration of $N_2$ gas may vary in the range of $5.92 \times 10^{17}$ to $1.20 \times 10^{19}$ $N_2$ molecules/$cm^3$.

Knowing this and $N_2$ molecular weight, one can calculate the quantity of $N_2$ gases which additionally may increase the nitrogen impurity content in graphite. Assuming, that cooling gases penetrate into the graphite structures and fill all open pores during reactor operation, for GR-280 grade graphite (having 1.65 g/$cm^3$ density and 17 % open porosity) this quantity is in the range of $2.8 \times 10^{-4}$ to $5.8 \times 10^{-3}$ %, while for GRP-2-125 grade graphite (having 1.85 g/$cm^3$ density and 14 % open porosity) it is in the range of $2.1 \times 10^{-4}$ to $4.2 \times 10^{-3}$ % of initial graphite mass for any possible cooling gas pressure and volumetric composition. Furthermore, assuming that cooling gases may fill not only open but and closed pores in the graphite, nitrogen impurities from cooling gases then may be in the range of $3.8 \times 10^{-4}$ to $7.8 \times 10^{-3}$ % for GR-280 grade graphite, and in the range of $2.3 \times 10^{-4}$ to $4.6 \times 10^{-3}$ % of initial GRP-2-125 grade graphite mass.

Generally, the cooling gases cannot easy penetrate into the closed graphite pores, thus assumption that these gases fill all pores volume seems unlike together with the fact, that e.g. the porosity of virgin (unirradiated) and of irradiated GRP-2-125 grade graphite is practically the same having the same proportions for open and closed pores volumes [11]. However, the dynamic of closed and open pores in the graphite under irradiation is not well known (do the pores stays as is or do the closed pores became open while open pores evolve into the closed, and etc.) and the possibility that closed pores in graphite may contain air (nitrogen comprises ~80 % volume in air) trapped in these pores during graphite manufacture processes, the assumption that all pores may contain nitrogen gas is still relevant.

Table 1 gives minimal and maximal calculated nitrogen concentrations in GR-280 and GRP-2-125 grades graphite (due to the cooling gas penetration into the graphite pores) for any possible cooling gas composition and operating pressure.

Table 1. Possible calculated nitrogen concentrations in GR-280 and GRP-2-125 grades graphite due to the cooling gas penetration into the graphite pores

| Cooling gas excess pressure, kPa | 0.49 | 1.96 |
|---|---|---|
| Nitrogen volumetric fraction in cooling gas, % | 5 | 100 |
| *Assuming, that cooling gas fills all open pores in graphite* | | |
| Nitrogen concentration in GR-280 graphite, % from initial graphite mass | $2.8\times10^{-4}$ | $5.8\times10^{-3}$ |
| Nitrogen concentration in GRP-2-125 graphite, % from initial graphite mass | $2.1\times10^{-4}$ | $4.2\times10^{-3}$ |
| *Assuming, that cooling gas fills all pores in graphite* | | |
| Nitrogen concentration in GR-280 graphite, % from initial graphite mass | $3.8\times10^{-4}$ | $7.8\times10^{-3}$ |
| Nitrogen concentration in GRP-2-125 graphite, % from initial graphite mass | $2.3\times10^{-4}$ | $4.6\times10^{-3}$ |

The ranges for possible calculated nitrogen concentrations in GRP-2-125 and GR-280 grades graphite due to cooling gas adsorption in all pores are marked respectively as interval "2" (orange) and "3" (green) in Fig. 9. The range of initial nitrogen impurity concentration in GR-280 graphite matrix from published sources is marked as interval "1" (black).

So, for the very conservative case, assuming maximal initial nitrogen concentration in the GR-280 grade graphite matrix ($7\times10^{-3}$ %) and maximal initial nitrogen concentration from cooling gases in the graphite pores ($7.8\times10^{-3}$ %), total $^{14}C$ activity in this graphite at the point of maximal thermal neutron flux is about $9.9\times10^{5}$ Bq/g, where $^{14}C$ generated from carbon activation comprise only ~7 %, while remaining 44 % and 49 % are for $^{14}C$ generated from nitrogen impurity in the graphite matrix and nitrogen gas in the graphite pores respectively. Similarly, assuming the same initial maximal nitrogen impurity concentration for GRP-2-125 grade graphite (the same as for GR-280) and maximal initial nitrogen concentration from cooling gases in the graphite pores ($4.6\times10^{-3}$ %), total $^{14}C$ activity in this graphite at the point of maximal thermal neutron flux is about $6.8\times10^{5}$ Bq/g, where $^{14}C$ generated from carbon activation comprise ~9 %, while remaining 55 % and 36 % are for $^{14}C$ generated respectively from nitrogen impurity in the graphite matrix and nitrogen gas in the graphite pores. However, it should be emphasised that above estimated activity of $^{14}C$ in the graphite pores is based on a conservative assumption that all generated $^{14}C$ remains in the pores (not escaping into the cooling gases).

The analysis also showed, that even at the point of maximal thermal neutron flux, the burn up of initial nitrogen impurity is not significant, i.e. the remaining nitrogen impurity mass after 21 year INPP Unit 1 reactor operation is still 96 % of the initial. Thus for modelling purposes, the fact that during reactor operation cooling gases circulates around the graphite structures and nitrogen concentration in the graphite pores may always be the same as initial, may be ignored, i.e. continuous feeding of material (graphite) with some quantity of nitrogen in order to keep it constant during graphite irradiation modelling is not necessary – it is enough to define only initial nitrogen impurity content.

From the point of view of irradiated graphite $^{14}C$ nuclide decontamination, analysis results may also be interpret in the way, that there can be 4 major fractions of $^{14}C$ release/removal from irradiated RBMK reactors graphite. The first, and likely the most difficult to remove is the fraction of $^{14}C$ coming from $^{13}C$ activation in graphite matrix, which can be in the order of $10^{4}$ Bq/g for both graphite grades. The second fraction is associated with nitrogen impurities, which are incorporated in the virgin graphite matrix, activation. This fraction of $^{14}C$ looks like also difficult removable from irradiated graphite and may be in the order up to $10^{5}$Bq/g depending on initial nitrogen impurity concentration. The third and fourth fractions are related to the nitrogen adsorption/penetration from cooling gases into the graphite pores and its activation. The fraction of $^{14}C$ being generated in the open pores may be in the order of $10^{5}$Bq/g in the most conservative case and in the closed pores it may be about 3 time lower for GR-280 grade graphite and about 7 times lower for GRP-2-125 grade graphite. These fractions of $^{14}C$

looks like the easiest fractions to remove (the fraction from open pores being more easy) during graphite decontamination, as generated $^{14}C$ is probably only adsorbed on the surfaces of the graphite pores and as free gases inside them, without being incorporated into the graphite matrix.

## CONCLUSIONS

Finalising performed analysis for RBMK-1500 reactor graphite several conclusion may be drawn:

- The obtained modelling results prove that thermal neutron flux is most important for $^{14}C$ generation in the graphite and that distribution of generated $^{14}C$ corresponds to the thermal neutron flux distribution;
- The activity of $^{14}C$ generated from carbon (raw graphite material) activation is in the order of $10^4$ Bq/g;
- Generation of $^{14}C$ from activation of initial nitrogen impurities in graphite matrix is linearly proportional to its quantity and at nitrogen concentration of $\sim 1 \times 10^{-3}$ % mass, $^{14}C$ generation from nitrogen activation equals the one from carbon activation;
- The very conservative estimation of possible nitrogen penetration from the cooling gasses into the graphite pores revealed, that nitrogen content in the graphite pores may be in the order of magnitude up to the $10^{-3}$ % of initial graphite mass, which is comparable to the maximal reported nitrogen impurity in the graphite matrix;
- $^{14}C$ generated from the activation of initial nitrogen impurity in the graphite matrix and from the activation of nitrogen trapped in the graphite pores may significantly influence total generated $^{14}C$ activity in graphite.

## AKNOWLEDGEMENTS

Funded by EC Project CARBOWASTE (FP7-211333), Lithuanian Science Development Program 01.01 and AISTDP.

## REFERENCES

1. Almenas, K.; Kaliatka, A.; Uspuras, E. *Ignalina RBMK-1500*: A source book. 2nd ed. Kaunas: Lithuanian Energy Institute, 1998. 196 p.
2. Smaizys A., Narkunas E., Poskas P. Modelling of activation processes for GR-280 graphite at Ignalina NPP. *Radiation protection dosimetry*, 2005, vol. 116, no. 1–4, p. 270–275.
3. Ancius, D.; et. al. Evaluation of the Activity of Irradiated Graphite in the Ignalina Nuclear Power Plant RBMK-1500 Reactor. *Nukleonika*, 2005, vol. 50, no. 3, p. 113−120.
4. Bylkin, B. K.; Davydova, G. B.; Krayushkin, A. V.; Shaposhnikov, V. A. Computational Estimates of the Radiation Characteristics of Irradiated Graphite after Final Shutdown of a Nuclear Power Plant with an RBMK Reactors. *Atomic Energy*, 2004, vol. 96, no. 6, p. 411–416.
5. Bylkin, B. K.; et. al. Induced Radioactivity and Waste Classification of Reactor Zone Components of the Chernobyl Nuclear Power Plant Unit 1 after Final Shutdown. *Nuclear Technology*, 2001, vol. 136, p. 76–88.
6. Virgilev Yu. S. Impurities in and Serviceability of Reactor Graphite. *Atomic Energy*, 1998, vol. 84, no. 1, p. 6–13.
7. Bushuev, A. V.; Zubarev, V. N.; Proshin, I. M. Impurity Composition and Content in Graphite from Commercial Reactors. *Atomic Energy*, 2002, vol. 92, no. 4, p. 331–335.
8. *Ignalina NPP Safety analysis Report*. Ignalina, 1996.

9. *Safety Analysis Report for INPP Unit 2*. Ignalina, 2003.
10. Hacker, P. J.; Neighbour, G. B.; Levinskas, R.; Milcius, D. Characterization of Ignalina NPP RBMK Reactors Graphite. *Materials Science*, 2001, no. 1, p. 62–66.
11. Bondarkov, M. D.; et. al. Activity Study of Graphite from the Chernobyl NPP Reactor. *Bulletin of the Russian Academy of Science: Physics*, 2009, no. 2, p. 261–265.